A static and "magic-angle" sample-spinning nuclear magnetic resonance spectroscopic study of ^{11}B in Si[B]. An analysis of spin–spin and spin–lattice relaxation behavior in the metallic state ☆

Jürgen Haase [a,b], Eric Oldfield [a,b] and Kirk Schmitt [c]

[a] *Department of Chemistry, University of Illinois at Urbana-Champaign, 505 South Mathews Avenue, Urbana, IL 61801, USA*
[b] *Materials Research Laboratory, University of Illinois at Urbana-Champaign, 104 South Goodwin, Urbana, IL 61801, USA*
[c] *Central Research Laboratories, Mobil Research and Development Corporation, Princeton, NJ 08540, USA*

Received 6 March 1992

We have investigated the signal intensity, lineshape, spin–lattice and spin–spin (spin-echo decay) relaxation behavior of ^{11}B nuclei in a Si[B] extrinsic semiconductor in the metallic state, as a function of magnetic field strength and temperature. We find that essentially all boron spins are in a highly symmetric environment, characterized by a mean nuclear quadrupole coupling constant (e^2qQ/h) of ≈ 12 kHz. The spin–lattice relaxation is Korringa like, with a $T_1T \approx 550$ s K, at both 5 and 300 K, indicating a mean Knight shift of ≈ 70 ppm. The spin–spin relaxation time, T_{2E}, is 25 ms at 8.45 T, independent of temperature, or magnetic field strength in the range 2.35 to 11.7 T, at 300 K. The T_{2E} value is in good agreement with the predictions of a model of homonuclear dipolar interactions within metallic Si[B] clusters.

1. Introduction

With the development of high-field "magic-angle" sample spinning (MAS) nuclear magnetic resonance (NMR) spectroscopic methods for the investigation of non-integral spin quadrupolar nuclei ($I=3/2$, $5/2$, ...) in inorganic solids, there has been renewed interest in investigating the spin–spin and spin–lattice relaxation behavior in these materials [1–5]. We have recently developed a model for spin–lattice relaxation of ^{17}O, ^{23}Na and ^{27}Al nuclei in zeolites in terms of fluctuating electric field gradients due to ion/water motion, and more recently we have developed a model for T_2 (spin-echo decay) behavior in a wide range of generally crystalline materials [3]. There is also increasing attention being paid to the use of T_2-like measurements by other groups, for example 2D NMR/nutation measurements of quadrupolar linewidths, ref. [4], and investigation of spin-echo decays, ref. [5], in less well defined materials, such as oxidic glasses [4] and semiconductors [5,6].

In two recent studies, Han and Kessemeier [5] and Han [6] investigated the ^{11}B NMR spin-echo decay behavior in several Si[B] semiconductors. They observed a rapid spin-echo decay in a highly B-doped material, which was interpreted in terms of the dominance of the second-order quadrupole interaction in governing spin–spin relaxation. We were intrigued by this new approach, and obtained a sample from Han and Kessemeier to try to determine, using much higher magnetic field strengths, the actual magnitude of e^2qQ/h, since second-order quadrupolar contributions are expected to be small at 11.7 T. Our results have yielded the surprisingly small e^2qQ/h value of ≈ 12 kHz for essentially all ^{11}B atoms in metallic state Si[B], and as we show below, T_1 and T_2 are both in accord with a simple model of metallic B clustering. Our results are only consistent with a very small amount of ^{11}B existing in a distorted, non-

Correspondence to: E. Oldfield, Department of Chemistry, University of Illinois at Urbana-Champaign, 505 South Mathews Avenue, Urbana, IL 61801, USA.

☆ This work was supported in part by the United States National Science Foundation Solid State Chemistry Program (grant DMR 88-14789) and by the Materials Research Laboratory Program (grant DMR 89-20538, JH).

cubic environment, which could contribute to the results of Han and Kessemeier [5]. In particular, we find that T_{2E} for most B nuclei is 25 ms, a value in agreement with that we deduce from our earlier model of homonuclear dipolar interactions [3].

2. Experimental

^{11}B static and MAS NMR measurements were made in Urbana using two "home-built" spectrometers, which operate using Oxford Instruments (Osney Mead, UK) 11.7 T 2.0 inch bore and 8.45 T 3.5 inch bore superconducting solenoid magnets, Nicolet (Madison, WI) model 1180 or 1280 computers interfaced to model 2090-IIIC (Explorer) transient recorders, and either Amplifier Research (Souderton, PA) or Henry Radio (Los Angeles, CA) radio frequency amplifiers. Static probes were of a "home-built" solenoidal coil design, while the MAS NMR probe was from Doty Scientific (Columbia, SC) Low temperature experiments were performed using an Oxford Instruments model CF1200 liquid helium refrigeration system. At Princeton, we used a hybrid Jeol/Chemagnetics 2.35 Tesla spectrometer, and a Chemagnetics (Fort Collins, CO) MAS NMR probe. The Si[B] sample was the kind gift of Dr. D.-Y. Han, and contained 2.2×10^{20} boron atoms per cubic centimeter. It was investigated as both intact wafers and as a fine powder, obtained by grinding in an agate mortar.

3. Results and discussion

We show by way of introduction in fig. 1 the static and MAS ^{11}B NMR spectra of Si[B] in a magnetic field of 11.7 T (corresponding to a ^{11}B resonance frequency of 160.36 MHz), obtained by using both single and spin-echo pulse excitation. The linewidth for the supper static spectrum, fig. 1A, is about 26 ppm (4.2 kHz), and we observed the same width for a batch of Si wafers as well as for the powder sample shown. The MAS NMR linewidth, fig. 1B, is slightly less than that of the static sample, while the spin-echo spectrum has about the same half-width as the static one-pulse spectrum, although some broad baseline features are absent, fig. 1C. Since the rotation frequency in the MAS NMR experiment was about 6 kHz, the very small effect of magic-angle spinning (a narrowing by a factor of about 1.4) shows that the static linewidth cannot be explained solely by an anisotropic shift, first-order quadrupolar interaction, or a dipolar interaction. Moreover, the second-order quadrupolar interaction, when dominating the observed linewidth, should lead to a decrease by a factor of 3.6 on MAS [7], and is thus also excluded as the major line-broadening mechanism. This conclusion is supported by the field-independence of the MAS linewidth, as shown by the 2.35 T result in fig. 1D. Thus, a distribution of isotropic frequency shifts must be the cause of the line broadening, and we show below that this distribution most likely arises from a distribution of Knight shifts in metallic B-containing clusters.

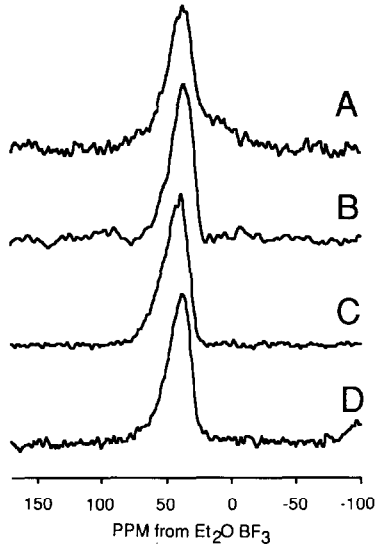

Fig. 1. ^{11}B NMR spectra of Si[B] at 300 K. (A) Static sample, single pulse experiment, 11.7 T. (B) MAS NMR spectrum, 6 kHz MAS rate, single pulse experiment, 11.7 T. (C) Spin-echo spectrum, $\tau=200$ μs, 11.7 T. (D) MAS NMR spectrum, 4.5 kHz MAS rate, single pulse experiment, 2.35 T.

In order to further investigate the spectra shown in fig. 1 it was necessary to find out whether all three transitions in the ^{11}B spin system were excited uniformly. The simplest and most reliable experiment for the estimation of any quadrupolar coupling is the dependence of the intensity of the resonance line upon the pulse length [8], a so-called nutation experiment. We show in fig. 2 the results of nutation

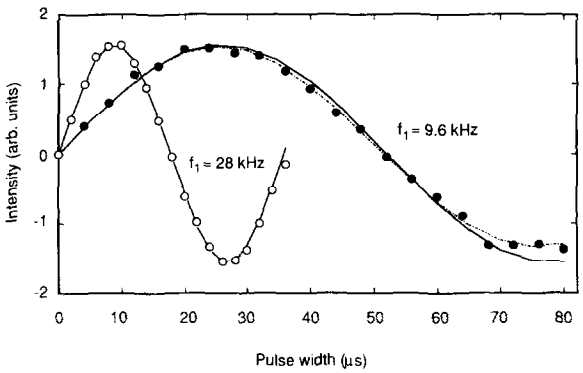

Fig. 2. 11.7 T ^{11}B NMR nutation behavior of Si[B] and aqueous boric acid, at two radiofrequency field strengths, together with a computer simulated result. (○) Semiconductor, $f_1 = 28$ kHz; solid line through data points, aqueous boric acid. (●) Semiconductor, $f_2 = 9.6$ kHz; solid line through data points, aqueous boric acid; broken line, theoretical nutation powder average for $f_1 = 9.6$ kHz, $e^2qQ/h \approx 12$ kHz, $\eta \approx 0$.

experiments for a static powder Si[B] sample and an aqueous H_3BO_3 solution, for two different amplitudes of the radio-frequency field, $2\pi f_1 = \omega_1 = \gamma B_1$. The results of fig. 2 clearly show that the pulse width dependence of the boron signal intensities corresponds to nonselective excitation [8]. Slight deviations from "liquid" behavior for very weak radiofrequency fields ($f_1 = 9.6$ kHz) can be explained by assuming a very small quadrupolar coupling, and as shown in fig. 2 we find good agreement between experiment and theory by taking a mean e^2qQ/h value of 12 kHz (η assumed $= 0$).

Inhomogeneity effects in f_1 over the sample volume can be excluded, since we used small samples in long, cylindrical coils. Moreover, the bandwidth of the NMR probe was the same for both the liquids and solids experiments (the quality factor being ≈ 70). Since e^2qQ/h is so small, quadrupolar effects during the excitation can be neglected in measurements of T_1 and T_2 [1–3], and we find, by using a π–$\pi/2$ (liquids) pulse sequence that $T_1 = 1.8 \pm 0.1$ s at 300 K, with the actual data points (not shown) fitting a single exponential. We discuss below the origin of this T_1 value. The linewidth and nutation results presented above were unexpected, based upon previous work on this sample [5].

We now consider the spin-echo decay behavior of the signal observed, and interpret the results in terms of the model for relaxation (spin-echo decay behavior) we have recently developed [3].

We show in fig. 3 the envelope of the spin-echo decay for an in-phase ($\pi/2|_x$–τ–$\pi|_x$) pulse sequence, as a function of temperature and magnetic field strength. We observe a rapidly decaying component with a time constant, T_{2E}, of about 50 ± 15 μs, and a much slower decaying component, having $T_{2E} = 25 \pm 3$ ms. For a 90° phase shifted ($\pi/2|_x$–τ–$\pi/2|_y$) pulse sequence similar results (not shown) were obtained. Only the time constant of the rapidly decaying component differed between the two pulse sequences, the T_{2E} for the phase-shifted pulse sequence being 100 ± 20 μs. We attribute this larger T_2 in the phase-shifted sequence to a partial refocusing of the satellite transitions, as expected for a first order interaction [3]. For both sequences, the rapidly decaying component accounts for about $60 \pm 10\%$ of the total intensity. The first, short T_2 component reflects the loss of the broad spectral component, as can be seen by comparing figs. 1A and 1C. After the rapid decay, fig. 3, the lineshape of the Fourier transform of the echo is almost identical to the MAS NMR lineshape, and is independent of magnetic field strength. The facts that the lineshapes and linewidths (in ppm) of the MAS NMR spectra are independent of magnetic field strength in the range 2.35 to 11.7 T, that the spin-echo decays are essentially superimposable at 2.35 and 11.7 T, the fact that 60% of the signal has a short T_2 and 40% a long T_2, and the observed nutation behavior (fig. 2), all strongly

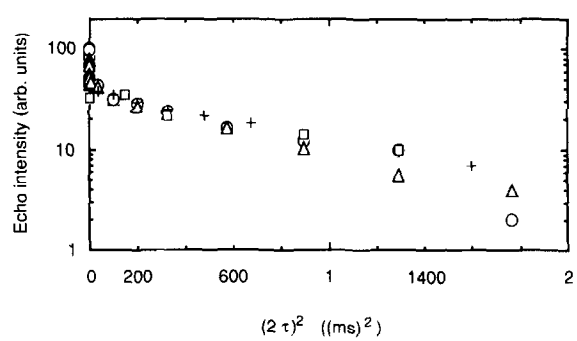

Fig. 3. Static spin-echo decay behavior for ^{11}B nuclei in Si[B] as a function of temperature and magnetic field strength. (○) 8.45 T, 300 K; (△) 8.45 T, 5 K; (+) 11.7 T, 300 K; (□) 2.35 T, 300 K. All spectra were obtained by using hard pulse [3] in-phase spin-echo radiofrequency excitation.

argue in favor of a small first order quadrupolar interaction combined with a frequency shift distribution, rather than a second-order quadrupolar interaction, as the dominant line-broadening mechanism in this sample. Thus, the broad component seen in the static spectrum, fig. 1A, arises from the satellite transitions of an $I=3/2$ nucleus, and corresponds to the 60($\pm$10)% rapidly decaying signal seen in the spin-echo decay, fig. 3. The narrower feature belongs to the 40% long T_2 component, fig. 3, which is the central ($+1/2$, $-1/2$) transition (theoretical intensity=40% for $I=3/2$, non-selective excitation). The field-independent linewidth, as discussed below, originates from a distribution of frequency shifts. If homonuclear dipolar interactions dominated the fast decay, the boron clustering required would inevitably cause severe lattice distortions, resulting in a large quadrupolar coupling, which is not observed.

Assuming a Gaussian distribution of quadrupolar coupling constants with a mean of 12 kHz and a standard deviation of 6 kHz, we calculated numerically the echo decay due to the first-order quadrupolar interaction for an in-phase pulse pair ($\pi/2|_x$–τ–$\pi|_x$), as well as for the sequence ($\pi/2|_x$–τ–$\pi/2|_y$). Our results confirmed the presence of the (60%) rapidly decaying components observed experimentally (with a T_2 of about 50 and 100 μs, respectively, data not shown).

As can be seen in fig. 3, the decay of the long-T_2 component is Gaussian, within experimental error. Furthermore, we obtain very good agreement between our T_{2E} results at 300 K at 2.35, 8.45 and 11.7 T, and between results at 5 and 300 K, at 8.45 T. Thus, given the lack of any field dependence, and the results of the nutation experiments (fig. 2), our results indicate the dominance of the homonuclear dipolar interaction in governing T_{2E} [3]. From the 1/e decay time of the slowly decaying component, $T_{2E}=25$ ms, we deduce a second moment for the corresponding Fourier transform of the Gaussian decay of $M_2=2/T_{2E}^2=3.2\times10^3\ \mathrm{s}^{-2}$.

Now, since the satellite transition frequencies are spread out due to quadrupolar coupling, dipolar spin-exchange is restricted to the central transition, slowing the spin-echo decay. The corresponding factor for the second moment is 0.455, for $I=3/2$ [3]. If, in addition, the observed MAS NMR linewidth represents a homogeneous broadening, resulting in neighboring boron spin having different resonance frequencies, then spin-exchange for even the central transition will be suppressed. This corresponds to a decrease of the experimentally observed second moment by a factor of 20, compared to the ordinary second moment for homonuclear dipolar interaction [3]. Thus, if the observed spin-echo decay is caused by dipolar interactions, a value of either about $3.2\times10^3/0.455=7\times10^3\ \mathrm{s}^{-2}$ or about $3.2\times10^3\times20=6.4\times10^4\ \mathrm{s}^{-2}$ is to be expected for the theoretical second moment of the homonuclear ^{11}B dipolar interaction.

The simplest approach for calculating the second moment of the homonuclear dipolar interaction is to assume the ^{11}B atoms form a simple cubic lattice. With an average ^{11}B–^{11}B distance of $d=1.78$ nm (from the known boron concentration) we find (ref. [9], p. 122, eq. (39′))

$$M_2=5.1\gamma^4\left(\frac{\mu_0}{4\pi}\right)^2\hbar^2 I(I+1)\frac{1}{d^6}\approx3.6\times10^3\ \mathrm{s}^{-2}. \quad (1)$$

Since the assumption of a simple cubic boron lattice is rather unlikely, we have also calculated second (and fourth) moments for random distributions of boron atoms, assuming that the boron atoms occupy regular sites in the silicon host lattice, as shown in fig. 4. Starting with the lattice structure of Si, we distributed the ^{11}B atoms randomly over the regular diamond lattice sites, taking the probability of finding a ^{11}B atom at a Si site to be 0.0035, corresponding to a boron concentration of $2.2\times10^{20}\ \mathrm{cm}^{-3}$.

A random distribution of boron atoms among the silicon sites would include some cases where boron clustering occurs. Since these dense boron clusters would represent a severe lattice distortion, we introduced a minimum ^{11}B–^{11}B distance, R, representing the distance of closest approach. We then computed the second moment (cf. ref. [9], p. 112, eq. (39));

$$M_{2E}=\tfrac{3}{5}\gamma^4\left(\frac{\mu_0}{4\pi}\right)^2\hbar^2 I(I+1)\sum_k\frac{1}{r_k^6}, \quad (2)$$

using a lattice sum over 10^3 nm^3 for 500 randomly created boron distributions, with $r>R$. The result is shown by the stars in fig. 4A. The chosen distances, R, are the next nearest neighbor distances in the diamond lattice, with the top left point in fig. 4A corresponding to the closest B–B distance allowed (the

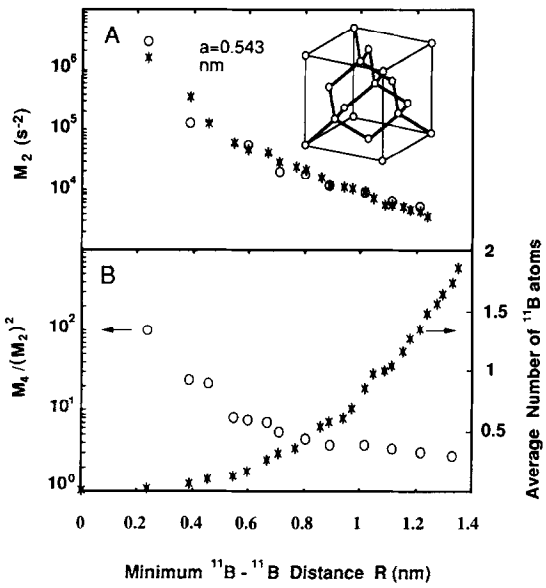

Fig. 4. Graphs showing the dependence of the second moment of the homonuclear dipolar interaction, M_2, the ratio of the fourth and second moment of the homonuclear dipolar interaction squared (M_4/M_2^2), and the average number of ^{11}B spins in a sphere with radius R, as a function of the minimum allowed ^{11}B–^{11}B distance (R). Inset: unit cell of the silicon lattice. (A) (*) Numerical calculations according to eq. (2); (O) numerical calculations according to ref. [9], p. 113, eq. (40). (B) (O) numerical calculations according to ref. [9], p. 113, eq. (40). (*) Number of ^{11}B atoms, as calculated from the number of nearest neighbours in the Si lattice multiplied by the average boron concentration (0.0035 per Si lattice site).

Si–Si spacing). In order to decide which R is appropriate for our Si[B] sample, we have utilized the fact that our echo decay is Gaussian, and for a Gaussian decay, a ratio of the fourth to (second moment)^2 is expected to be 3 (ref. [9], p. 113, eq. (40)). We calculated numerically the fourth moment of the ^{11}B–^{11}B interaction (ref. [9], p. 113, eq. (40)), averaging 400 different boron distributions. As a check of the numerical procedure, and in order to provide an estimate of the adequacy of the powder average, we show in fig. 4A the second moments (circles) from these latter calculations. Fig. 4B (circles) shows the ratio of the fourth moment divided by the square of the second moment. For $M_4/(M_2)^2=3.0$, we find that $R \geqslant 1$ nm, a distance which corresponds to only ≈ 1 boron atom in an $R=1$ nm radius sphere, fig. 4B (*). These results are consistent with a second moment of $<10^4$ s^{-2} (for $R \geqslant 1$ nm, fig. 4A), which when compared with the experimental result, leads to the conclusion that spin-flipping in the central transition is not suppressed. We thus conclude that boron spins exist in clusters, with the frequency shift of each atom in a cluster being equivalent, but with the frequency shifts of different clusters (containing different numbers of boron atoms) varying. Within each cluster, the T_{2E} values are essentially constant. This picture is quite consistent with previous work on metallic phase semiconductors [10–14], and as we discuss below, it is due to a distribution of Knight shifted resonances, which gives rise to the asymmetric line shapes (fig. 1).

We now consider the question of how much boron in our sample can be accounted for from the NMR spectra. The expected boron concentration in our sample was stated to be 2.2×10^{20} cm^{-3}, which is 1640 ppm, a result consistent with two independent determinations carried out in our laboratories (1500 ppm, 1600 ppm) using microanalysis. Using NMR, we quantitated the total boron spin-echo intensity against three standard samples of aqueous boric acid, fitting the experimental intensities to the echo-decay curve shown in fig. 3, and found a total boron concentration of 1450 ± 100 ppm. Thus, our results indicate that within the limit of experimental error ($\pm8\%$) all ^{11}B spin contribute to the NMR signal.

4. Knight shift effects

As we briefly discussed above, the ^{11}B NMR line narrows only slightly upon MAS, and has an essentially field-independent width (in ppm), in the 2.35–11.7 T range of magnetic field strengths. From the spin-echo decay we found for the second moment of the homonuclear dipolar interaction $M_2\approx7\times10^3$ s^{-2}, which corresponds to a Gaussian linewidth of $\Delta\nu\approx30$ Hz ($\Delta\nu=\pi^{-1}\sqrt{2\ln2}\sqrt{M_2}$). Since the observed width is so much greater, an inhomogeneous broadening must be responsible.

A purely chemical shift dispersion seems unlikely, and indeed the question of the origin of the ^{29}Si, ^{11}B and ^{31}P linewidths in extrinsic semiconductors has been investigated previously [10–12]. However, a detailed analysis of the ^{11}B NMR resonance in Si[B] has not yet been reported, although studies of ^{29}Si in Si[B] and of ^{29}Si and ^{31}P in n-type Si[P] samples

[11] show that the Si and P lineshapes are determined, at high dopant levels, by interactions with conduction electrons.

Strong evidence for the influence of conduction electrons comes from measurement of spin–lattice relaxation rates. We find at room temperature a mean T_1 of 1.8 s, while at 5 K T_1 has increased to about 110 s, leading to a T_1T of about 550 s K at both temperatures. This indicates Korringa type relaxation, and from the Korringa equation,

$$K^2T_1T\left(\frac{\gamma_n}{\gamma_e}\right)^2\frac{4\pi k_B}{\hbar}=1\,, \tag{3}$$

we deduce a mean Knight shift, K, of about 68 ppm, in the independent electron approximation.

Progressive saturation of the ^{11}B resonance at 11.7 T and 300 K ($\pi/2$–Δ–π echo sequence, $\Delta=300$ μs; repetition time of the experiment varied from 15 to 0.1 s) revealed only a slight change of the linewidth of the Fourier transform of the echo. The resonance line shifted by about 20% of the total linewidth to higher frequency by decreasing the repetition time, while the low-frequency side of the line remained unaffected. This change indicates that the high-frequency side of the line corresponds to spins with a somewhat bigger Knight shift ($T_1 \propto 1/K^2$). Due to the quadratic dependence of T_1 on the Knight shift, K, and the relatively small change in the linewidth for the case of fast recycling, the distribution of Knight shifts has to be much smaller than its mean value. A mean Knight shift of about 70 ppm, as deduced from the Korringa law, and a distribution given by the linewidth of the central transition (about 20 ppm) account for the observed T_1 effects.

A linewidth caused by a distribution of Knight shifts for the ^{31}P resonance in Si[P] had been suggested by Sundford and Holcomb [10]. These authors compared the line shape of the ^{31}P resonance with a Poisson distribution. They argued that due to the random distribution of impurity P atoms in the Si lattice, the impurity electron density, N, is proportional of the Knight shift, K. From the Bohr radius of an impurity electron (or hole) a critical volume for the formation of the metallic state can be defined and the number of impurity atoms in this critical volume is given by the Poisson distribution. The resonance shift of the NMR line is now a function of the number of impurity atoms in the critical volume. These authors found that the high-frequency side of the ^{31}P resonance line could be fitted to a Poisson distribution, but the intensity on the low-frequency side of the resonance decreased much more rapidly than expected from the Poisson distribution.

For the ^{11}B resonance we find similar results when comparing the lineshape with a Poisson distribution. However, assuming this model to be accurate, a ^{11}B intensity of up to about 30% should be missing in the NMR spectra (similar to the reported ^{31}P results). Since these spins are not relaxed by the conduction electrons, their relaxation times could be very long. We thus increased the recycle delay up to 500 s, but no additional intensity could be observed, consistent with our NMR results on boron quantitation. Since we find no evidence for the "missing" 30% boron, our results suggest that the previous model [10] of metallic clusters is incomplete, or at least, not applicable to ^{11}B. Also, our analysis of the second and fourth moments, which support an inhomogeneous line broadening, suggests that the smallest boron distance is about 1 nm. Such a non-random boron distribution diminishes the amount of the "missing" intensity, since it modifies the Poisson distribution.

5. Conclusions

The results we have obtained above indicate the following: First, the quantitative ^{11}B NMR results show that essentially all boron spins are observed in our NMR spectra. Second, the mean nuclear quadrupole coupling constant is about 12 kHz, consistent with the general expectation of a small e^2qQ/h due to location of B atoms on sites of high symmetry in the Si lattice. Third, we obtain a T_{2E} value of 25 ms, independent of temperature (at 8.45 T) and magnetic field strength (at 300 K, and between 2.35 and 11.7 T), and this T_{2E} is that which is expected from our model of homonuclear dipolar interactions [3]. Fourth, the T_1T value obtained, $T_1T=550$ s K, is the same as that obtained by previous workers [10,11], and does not vary between 5 and 300 K. Fifth, the observed lineshape is generally consistent with previous ideas of a critical volume for metallic behavior, and previous results for ^{29}Si and ^{31}P in Si[P] [10–12], although the quantitative observation of

essentially all ^{11}B suggests that the B distribution is not completely random.

Overall, our results indicate that most B nuclei in metallic Si[B] are on highly symmetric BSi_4 lattice sites, that Korringa relaxation dominates T_1, that the lineshapes are governed by distribution of Knight shifts, and that the ^{11}B spin-echo NMR behavior is governed by homonuclear dipolar interactions [3].

Acknowledgement

We thank D.-Y. Han for providing the Si[B] sample, and helpful discussions, and Jay Shore, for performing the low-temperature experiments.

References

[1] J. Haase, K.D. Park, K. Guo, H.K.C. Timken and E. Oldfield, J. Phys. Chem. 95 (1991) 6996.
[2] J. Haase, H. Pfeifer, W. Oehme and J. Klinowski, Chem. Phys. Letters 150 (1988) 189.
[3] J. Haase and E. Oldfield, J. Magn. Res., submitted for publication.
[4] J. Dolinsek, J. Magn. Res. 92 (1991) 312.
[5] D.-Y. Han and H. Kessemeier, Phys. Rev. Letters 67 (1991) 346.
[6] D.-Y. Han, Ph.D. Thesis, University of North Carolina at Chapel Hill (1990).
[7] D. Freude, J. Haase, J. Klinowski, T.A. Carpenter and G. Ronikier, Chem. Phys. Letters 119 (1985) 365.
[8] D. Fenzke, D. Freude, T. Fröhlich and J. Haase, Chem. Phys. Letters 111 (1984) 171.
[9] A. Abragam, Principles of nuclear magnetism (Oxford Univ. Press, Oxford, 1961).
[10] R.K. Sundfors and D.F. Holcomb, Phys. Rev. 136 (1964) A810.
[11] G.C. Brown and D.F. Holcomb, Phys. Rev. B 10 (1974) 3394.
[12] W. Sasaki, S. Ikehata and S. Kobayashi, J. Phys. Soc. Japan 36 (1974) 1377.